Eur Biophys J (2000) 28: 611–620

ARTICLE

Claudia M. Kacher · Ingrid M. Weiss
Russell J. Stewart · Christoph F. Schmidt
Paul K. Hansma · Manfred Radmacher · Monika Fritz

Imaging microtubules and kinesin decorated microtubules using tapping mode atomic force microscopy in fluids

Received: 23 February 1999 / Revised version: 19 July 1999 / Accepted: 17 August 1999

Abstract The atomic force microscope has been used to investigate microtubules and kinesin decorated microtubules in aqueous solution adsorbed onto a solid substrate. The netto negatively charged microtubules did not adsorb to negatively charged solid surfaces but to glass covalently coated with the highly positively charged silane trimethoxysilylpropyldiethylenetriamine (DETA) or a lipid bilayer of 1,2-dipalmitoyl-3-dimethylammoniumpropane. Using electron beam deposited tips for microtubules adsorbed on DETA, single protofilaments could be observed showing that the resolution is up to 5 nm. Under conditions where the silane coated surfaces are hydrophobic, microtubules opened, presumably at the seam, whose stability is lower than that of the bonds between the other protofilaments. This led to a "sheet" with a width of about 100 nm firmly attached to the surface. Microtubules decorated with a stoichiometric low amount of kinesin molecules in the presence of the non-hydrolyzable ATP-analog 5′-adenylylimidodiphosphate could also be adsorbed onto silane-coated glass. Imaging was very stable and the molecules did not show any scan-induced deformation even after hundreds of scans with a scan frequency of 100 Hz.

Key words Kinesin · Microtubules · Atomic force microscopy

C.M. Kacher · I.M. Weiss · M. Fritz (✉)
Physik Department der TU-München,
Institut für Biophysik E22,
James-Franck-Strasse, D-85747 Garching, Germany
e-mail: mfritz@physik.tu-muenchen.de

R.J. Stewart
Bioengineering Department, University of Utah,
Salt Lake City, UT 84112, USA

C.F. Schmidt
Department of Biophysics and Physics of Complex Systems,
Vrije Universiteit Amsterdam,
1081 HV Amsterdam, The Netherlands

P.K. Hansma
Department of Physics,
University of California Santa Barbara, CA 93106, USA

M. Radmacher
Sektion Physik der LMU München,
Institut für Angewandte Physik, Amalienstrasse 54,
D-80799 Munich, Germany

Introduction

Since its invention in 1986 the atomic force microscope (AFM) (Binnig et al. 1986) has become a widely used instrument for biological applications. Living cells have been imaged (Radmacher et al. 1992; Fritz et al. 1994; Hoh and Schoenenberger 1994) and mechanical properties of intact platelets have been observed (Radmacher et al. 1996). Also, imaging of two-dimensional crystals of proteins became possible: gap junctions have been resolved in aqueous solution (Hoh et al. 1993) as well as bacteriorhodopsin (Müller et al. 1995b). Other molecules like DNA could be observed with a resolution down to the helix turn (Bezanilla et al. 1995). Imaging single randomly distributed protein molecules physically (Yang et al. 1993) or chemically (Karrasch et al. 1993) bound to a surface has been challenging because of the relatively high lateral forces on the soft material. A new imaging mode, the tapping mode in liquids (Hansma et al. 1994), has been invented and made it possible to image single protein molecules in buffer solution. Actin filaments (Fritz et al. 1995b) and microtubules (Fritz et al. 1995a) could be investigated with high resolution. Moreover, even dynamical aspects of enzymes could be shown: the degradation of DNA molecules loosely adsorbed on mica (Bezanilla et al. 1994) and the activity of lysozyme molecules during hydrolysis of their substrate (Radmacher et al. 1994). This shows that the AFM opened a new field to investigate biological molecules: the investigation of biological samples with high resolution in their natural environment, which is the aqueous solution. We show here that AFM operated in tapping mode in liquid is

capable of resolving single cytoskeletal proteins in buffer solution with a resolution of about 5 nm.

Microtubules are protein polymers which form long, stiff rods in cells and act in this conformation as "railways" for motor proteins like kinesin, dynein or ncd (for an overview, see Hyams and Lloyd 1994). They are required for various processes like the separation of genetic material and intracellular transport. They are dynamic structures, permanently undergoing processes like assembly and disassembly. Reconstituted microtubules consist of 13–18 protofilaments, depending on the buffer conditions (Brinkley 1997). In living cells, microtubules consist of 13–14 protofilaments forming a hollow cylinder with an outer diameter of about 30 nm. The elongated protofilaments bind to each other, forming the hollow cylinder. The axial shift between adjacent protofilaments is 0.92 nm for a 13-protofilament microtubule and 0.86 nm for a 14-protofilament microtubule. In these protofilaments the tubulin monomers consisting of α- and β-subunits, each with a relative molecular mass of about 50 kDa, are bound to each other in a head-to-tail-like fashion, each subunit having a diameter of about 4 nm. Thus a tubulin monomer is a small rod of 8 nm in length and 4 nm width. The surface lattice of the microtubules shows a helical structure with a 3-start helix, 13 protofilaments and a B-lattice (Mandelkow et al. 1986). This means that there is a discontinuity in the microtubule lattice called a "seam" (Mandelkow et al. 1986; Metoz and Wade 1997; Wade and Hyman 1997). The stability of the seam is lower than that of the bonds between the other protofilaments. We show here that under certain conditions the microtubules remain as hollow cylinders at the surface. At the very end of microtubules, where the upper part of the cylinder is broken, we can image the inside of the microtubule showing that it is rougher than the outside. Interaction forces between microtubules and a hydrophobic surface lead to microtubule "sheets" lying flat on the surface. The microtubules may open, presumably at the seam, and adsorb as a flat "sheet" on the solid support.

Kinesin molecules are motor proteins consisting of two head domains, an α-helical coiled stalk and a tail domain which can bind to a load. It is a plus-end directed motor protein, a microtubule-activated adenosine triphosphatase (ATPase) (Bloom and Endow 1994; Hirokawa 1998). The 380 kDa kinesin molecule consists of two 120 kDa heavy chains and two 64 kDa light chains which constitute the fan-like end where the load can bind (Vale et al. 1985; Bloom et al. 1988). The head or motor domain has a size of about $6 \times 3.5 \times 3$ nm and the total length of kinesin is 80 nm. These motor domains bind to microtubules and carry a load at the tail group as membrane-bound compartments filled with freshly synthesized material from the nucleus. As it is moving along a microtubule, steps of 8 nm have been measured using optical tweezers (Svoboda et al. 1993; Block 1997). This is consistent with the length of a tubulin monomer (α- and β-subunit) in the microtubule. It has been shown that the kinesin head is spread over both subunits but is more concentrated over one subunit (Hirose et al. 1995; Kikkawa et al. 1995), which is the β-tubulin (Hoenger et al. 1998). The stoichiometry is one head bound to one tubulin heterodimer (Thormählen et al. 1998). We show here that AFM can observe microtubules decorated with kinesin molecules with a resolution up to 5 nm. All images shown were acquired in aqueous solution.

Measurements with the AFM are prone to an artifact called "tip broadening" which is due to the finite size of the tip. The broadening of a structure by the imaging tip depends on the geometry of the tip (see text of Results and discussion section and Fig. 3). The dimensions of the molecules measured by other methods like X-ray diffraction, electron diffraction or electron microscopy are given in Table 1 (Wade and Hyman 1997; Hoenger et al. 1998).

Materials and methods

Preparation of the silane and lipid-coated solid support

Glass cover slips (Plano, Wetzlar, Germany), 13 and 11 mm in diameter, were cleaned thoroughly before coating them with silane. First they were incubated for 2 h in Piranha solution (70% concentrated H_2SO_4, 30% concentrated H_2O_2), then they were rinsed several times with deionized water (MilliQ, Millipore System, Eugene, Ore., USA) and three times ultrasonicated in deionized water for 3 min. They were silanized with trimethoxysilylpropyldiethylenetriamine (DETA, United Chemical Technologies, Bristol, Pa., USA); 1% DETA was hydrolyzed in 1 mM acetic acid for 5 min. The cover slips were immersed in this solution for 2 min, rinsed in deionized water and sonicated for 2 min. Finally, they were dried and cured for 15 min at 150 °C. The DETA surface has a hydrophilic appearance. DETA surfaces become hydrophobic after about 4 weeks of storage. This type of surface is called "outdated DETA" here.

For the lipid-coated solid support a vesicle suspension of the lipid 1,2-dipalmitoyl-3-dimethylammoniumpropane (DPDAP, Avanti Polar Lipids, Birmingham, Ala., USA) was used. The preparation of the vesicle suspension was as follows. DPDAP (10 mg) was dissolved in chloroform (1 ml) and the chloroform was evaporated completely. Deionized water (2 ml) (MilliQ) was added to

Table 1 Approximate dimensions of microtubules and kinesin and their subunits

Molecule	Size
Tubulin heterodimer	$8 \times 4 \times 4$ nm
Protofilament	4 nm diameter
Microtubule	30 nm outer diameter
Kinesin headgroups	$6 \times 3.5 \times 3$ nm
Kinesin dimer	80 nm length

the totally dried out lipids and incubated at 40 °C for 2 h for soaking. Then the suspension was sonicated in a trunk sonicater (UW 70, Bachhofer, Reutlingen, Germany) for 10 min to obtain small vesicles (less than 500 nm in diameter). Vesicle fusion on mica was done for 12 h at 70 °C. The sample was rinsed in deionized water to remove excess material and was then used for the adsorption of microtubules. The sample was never allowed to dry.

Preparation of microtubules

Tubulin was purified from pig brain following the procedure of Williams and Lee (1982) and aliquots of 100 µl (at a concentration of 4 mg/ml) were stored at −80 °C. The aliquots were thawed on ice for 1 h and centrifuged at 100,000 *g* at 4 °C to remove contaminants and polymerized material. Then 1.2 mg/ml tubulin was polymerized in PEM 50 buffer (50 mM PIPES = piperazine-*N*, *N*′-bis[2-ethanesulfonic acid], 1 mM EGTA, 2 mM $MgCl_2$, 2 mM NaN_3, pH 6.8 with 10 µM taxol) at 37 °C for 30 min. The tubulin solution was allowed to polymerize for an additional 12 h at room temperature after it was removed from the waterbath. The polymer solution was centrifuged for 30 min at 14,000 rpm (room temperature, Eppendorf, 5415 C, table top centrifuge) to remove unpolymerized tubulin. The supernatant was discarded and replaced by the same volume of pure PEM 50 buffer at pH 6.8 and 3 µM taxol and the pellet was resuspended. Then 10 µl of this solution were adsorbed for 10 s on DETA-coated cover slips or on DPDAP coated mica (see above) and rinsed vigorously with PEM 50 buffer containing 3 µM taxol. The sample was never allowed to dry.

Preparation of kinesin-decorated microtubules

Microtubules were prepared as described above. After the centrifugation at 14,000 rpm with the table top centrifuge, 10 µM 5′-adenylylimidodiphosphate (AMP-PNP) and 0.5 mg/ml kinesin were added. The kinesin construct K595H (Yang et al. 1990) was used for the experiments. This is a mutant from *Drosophila* containing 595 amino acids expressed in *Escherichia coli* with a molecular weight of 70 kDa. The protein solution was frozen in liquid nitrogen until it was used for the decoration experiments. After carefully thawing the solution it was incubated with the microtubules for 2 h prior to imaging with the AFM. Then 10 µl of this solution were adsorbed for 10 s on DETA-coated cover slips (see above) and rinsed vigorously with PEM 50 buffer containing 3 µM taxol. The sample was never allowed to dry.

AFM imaging

AFM was performed with a commercial microscope (Nanoscope III A, Digital Instruments, Santa Barbara, Calif., USA), which could be operated in tapping mode in liquids (Hansma et al. 1994). In this mode, less damage occurs to soft samples. The cantilever is modulated sinusoidally at high frequencies (between 8 and 35 KHz, amplitude about 5 nm). The cantilever response depends on the distance between tip and sample. The cantilever response is used as the input to a feedback loop, adjusting the piezo height such that this amplitude stays constant while tracing the surface. This mode is analogous to the constant deflection mode in conventional AFM. Various types of tips were used: Si_3N_4 tips (oriented twin tips, 200 µm long and 12 µm wide, Digital Instruments, Santa Barbara, Calif., USA and microlevers 180 µm long, 18 µm wide, Park Scientific Instruments, Sunnyvale, Calif., USA) and silicon tips (Ultralevers, 180 µm long, 18 µm wide, Park Scientific Instruments). The tapping frequencies ranged from 8 to 35 kHz.

Results and discussion

After the invention of the tapping mode in liquids for AFM imaging (Hansma et al. 1994) it became possible to image even single proteins in buffer solution. The resolution varies depending on the protein (Fritz et al. 1995b; Schabert and Rabe 1996), the pH and the ionic strength of buffer solution used. For AFM imaging, samples have to be immobilized at a surface. This surface should be very clean and flat. The sample can be immobilized by chemical or physical interactions. For chemical covalent linking of a molecule to a surface there has to be (in most cases) at least one additional layer between the solid surface and the sample (Karrasch et al. 1993, 1994). This leads usually to a softer sample which might reduce resolution. For physical bonds, electrostatic forces are the most promising interactions to bind a biological sample to a surface. As most of the available flat solid surfaces for AFM imaging are negatively charged, a low pH it is useful to make the proteins more positively charged. Also a low concentration of the electrolyte in the buffer solution favors the immobilization of proteins. As the function of proteins depends also on certain buffer conditions (e.g. most of them favor pH 7), one has to find conditions which serve the function of increasing the electrostatic interactions of the proteins with the support and also keep the proteins native and functional.

Resolution of AFM images

The lateral and vertical resolution in AFM depends on several factors. One of them is the tip geometry. This will be discussed in the first "microtubules" section below. Other factors are the applied or inherent forces between tip and sample. Electrostatic and/or van der Waals forces affect the minimum force which can be applied to the sample. Electrostatic forces influence, for example,

the adsorption strength of a molecule and therefore the lateral and vertical resolution. High attractive van der Waals forces between the tip and a soft sample would very likely lead to a lower resolution than small van der Waals forces because they push the tip down to the sample.

Hence the resolution in AFM imaging depends on the sample, the buffer conditions and the tip which is used. This is different to the resolution following Abbe's equation for light microscopy. However, the AFM tip not only "detects" topographic structures but resolves true distances between structures.

The supporting silane surface

Several supports with different surface properties were tried to adsorb microtubules. At pH 7, microtubules are netto negatively charged hollow cylinders which do not adhere strongly enough to negatively charged surfaces like mica, glass or silicon oxide for AFM imaging in buffer solution (Vinckier et al. 1995). Glass surfaces can be coated with different silanes with a variety of different headgroups. We tried hydrophobic silanes and positively charged silanes. All of them make a covalent contact to the glass surface and polymerize laterally to form an almost crystalline layer on the surface. This is very important in order to obtain a rigid and dense surface coating. A soft layer underneath the adsorbed microtubules would decrease the resolution. Dimethyldichlorosilane and octadecyltrichlorosilane as hydrophobic substrates did not help to adsorb the microtubules. 4-Aminobutyldimethylmethoxysilane, a silane with a headgroup with one positive charge, was also not a useful substrate to immobilize the microtubules. Only a very dense packing of positive charges made it possible to bind the microtubules to the surface for AFM imaging: a cover glass coated with the silane DETA. The headgroup carries three amino groups which are all positively charged at the given pH of 6.8. The silane molecules build a dense layer on the glass surface, assuming that they are polymerized laterally. In Fig. 1 an AFM image of one of our samples of a typical surface coated with DETA is shown; in Fig. 1A an overview of the surface is shown. The entire surface is coated and there are no visible holes or defects on this scale. In Fig. 1B a zoom-in on the same surface is shown. A crystalline lattice of DETA molecules

Fig. 2A–D Microtubules adsorbed onto DETA imaged in buffer solution by AFM. The imaging was done in tapping mode. **A** Overview in the height signal: the silane DETA bound to a glass surface has a head group with three positive charges, making the surface densely positively charged. The negatively charged microtubules adhere nicely to the silane. They have a height of 30 nm which corresponds to the diameter of microtubules. The imaging was done with a silicon nitride cantilever. **B** Error signal of a close-up view of a microtubule. This shows the small corrugations on the molecules; there is no information on the height of the structures. The *arrows* indicate the protofilaments. The imaging was done with a silicon nitride cantilever with an ebd tip. **C** Overview of microtubules in the error signal where part of the upper half of the cylinder is broken (*arrow*). The imaging was done with a silicon nitride cantilever with an ebd tip. **D** Close-up view in the error signal of a microtubule where the upper part is broken. This makes it possible to look "inside" the microtubule. The inner surface is more rugged (*arrows*) than the outer one. The imaging was done with a silicon nitride cantilever with an ebd tip

Fig. 1A, B AFM images of a DETA-coated cover glass. The imaging was done in contact mode with a silicon nitride cantilever. **A** Large scale image of the surface. Note that there are no visible defects or holes on this scale. The root mean square is 0.3 nm. **B** Molecular resolution on a zoom-in of the same surface. There is a thermal drift on part of the sample which can be seen in the parallel lines at the lower third of the image. The upper part shows the silane molecules in a dense packing arrangement

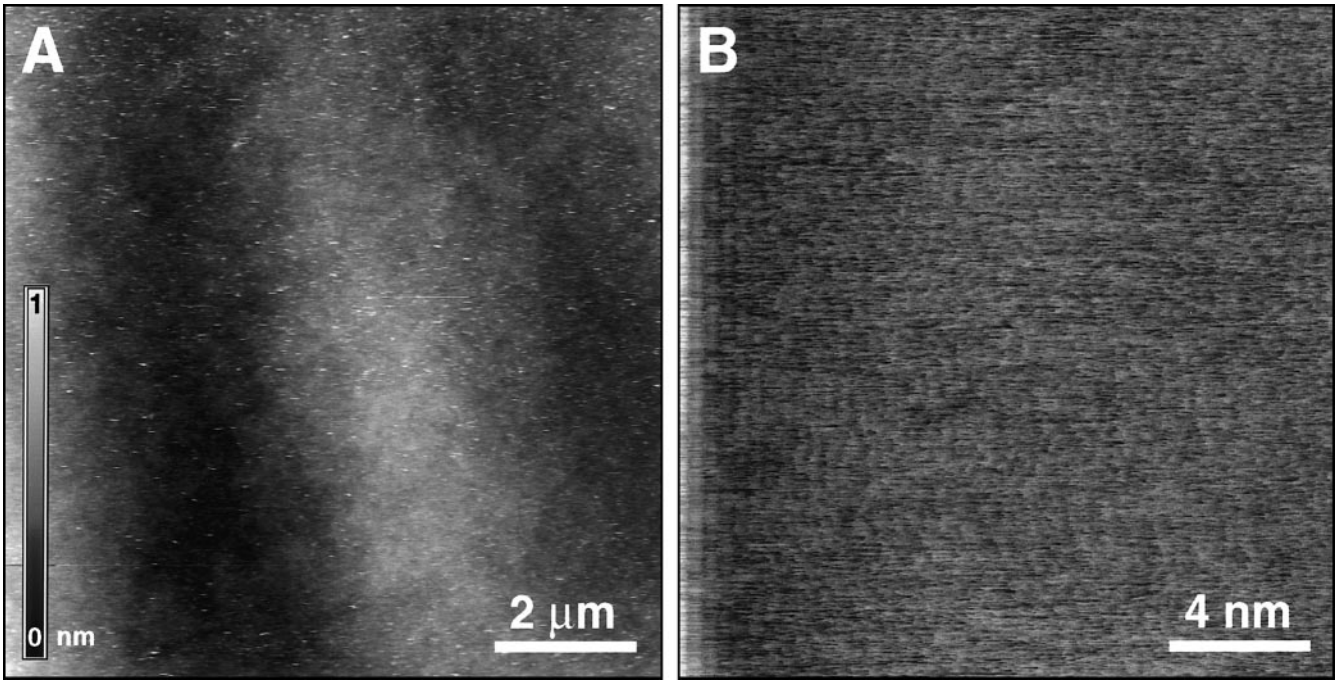

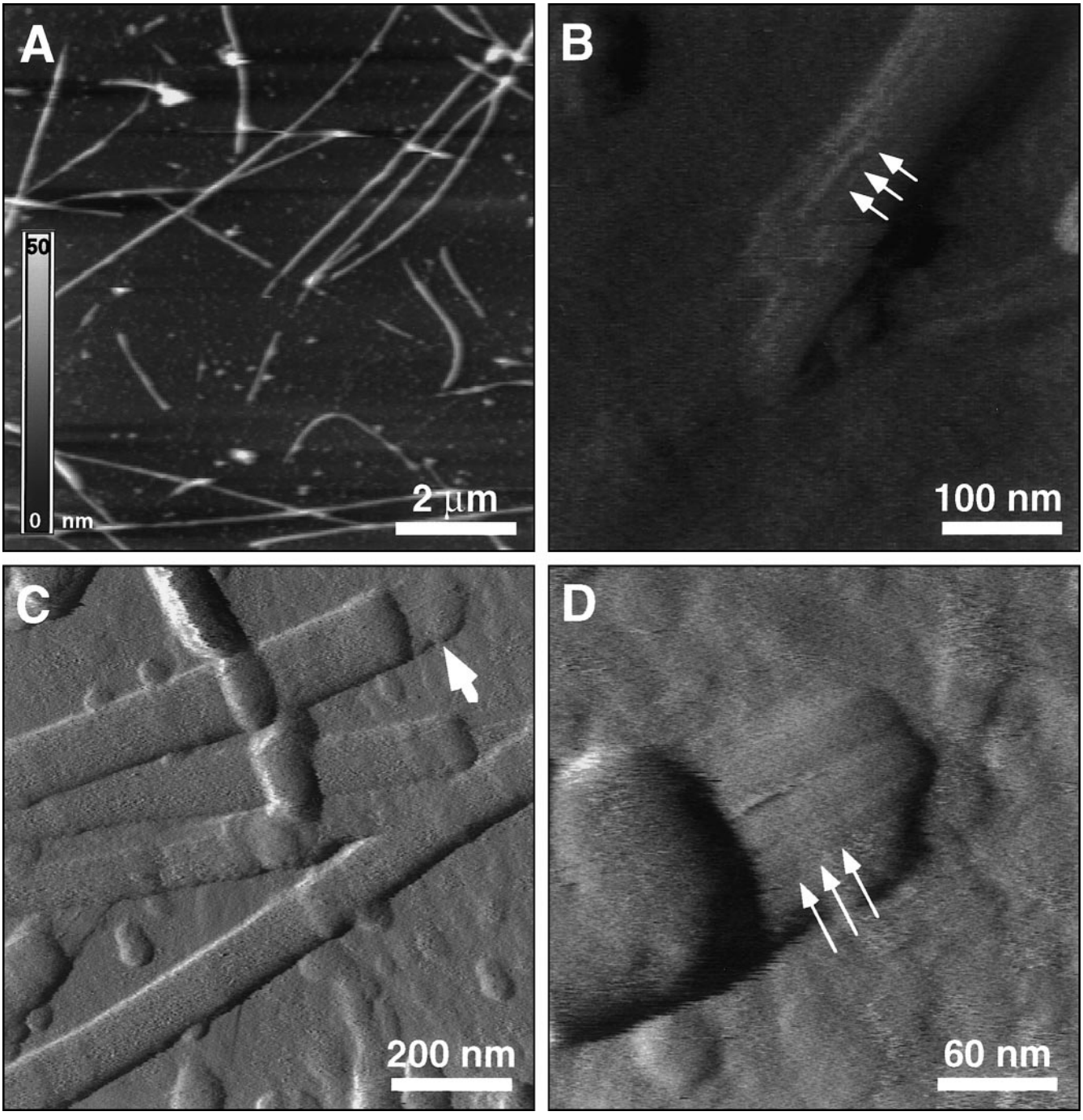

is slightly visible, indicating a very dense packing of positive charges.

The silane surface described above and a lipid bilayer of positively charged lipids (described in the Materials and methods section) can be used to immobilize microtubules.

Microtubules adhere to a positively charged silane or lipid

Microtubules stabilized with taxol bind to the positively charged silane DETA. In order to obtain a good distribution of filaments bound to the surface, a high concentration of microtubules has to be incubated at the surface for a very short time. Using a lower concentration than 1 mg/ml leads to a surface covered with tubulin monomers and there is no space left for the microtubules. This is because the smaller monomers diffuse much faster than the larger polymers. In order not to overload the sample because of the high concentration of proteins the incubation time has to be only a few seconds. Usually single globular proteins are adsorbed at a concentration of about 1 μg/ml to a surface and the incubation time is 30 min. In Fig. 2A an overview of randomly distributed filaments is shown.

Microtubules are very rigid structures with a persistence length of 2 mm; thus they should not bend on the length scale of several micrometers. However, occasionally we observed bending on the length scale of a few micrometers (e.g. Fig. 2A, lower right). The microtubules imaged in AFM tapping mode in liquids do have a height of about 30 nm, which corresponds very well to electron microscopic data of cross-sections of microtubules (Mandelkow et al. 1986). On this scale there is no substructure visible and we could not resolve any substructure on a smaller scale with tips usually used for AFM imaging like silicon nitride or silicon tips (see Materials and methods section). The apparent diameter of the microtubules is between 80 and 120 nm. This is due to the "tip broadening" which can be attributed to the finite size of the tip raster scanning the surface (Fig. 3).

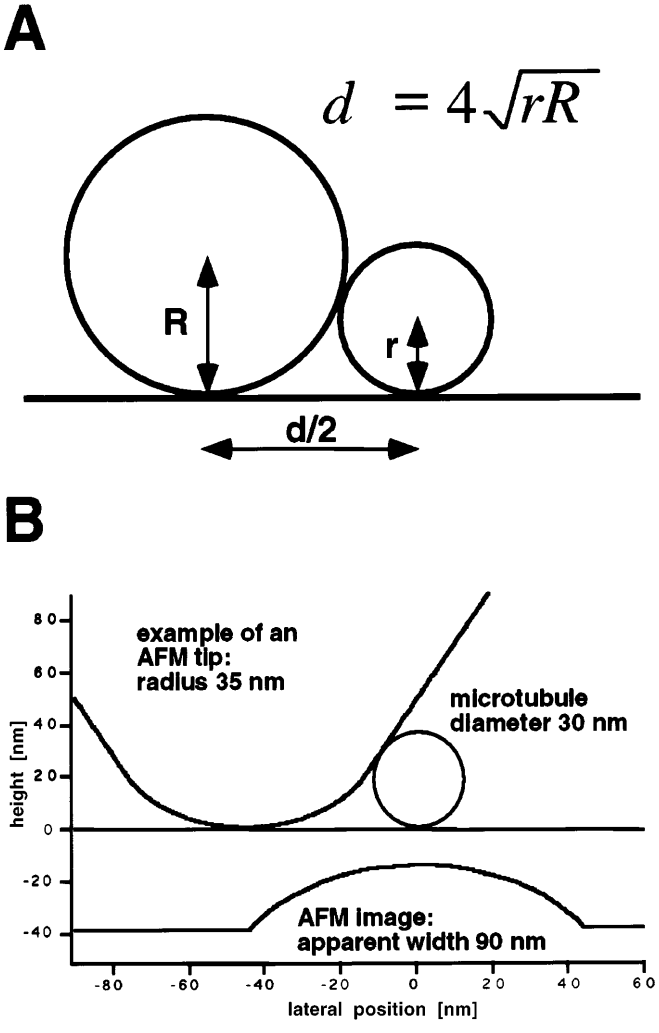

Fig. 3A, B Sketch of an AFM tip scanning a sample. **A** Sketch of an AFM tip with a radius R scanning a sample with a radius r. The apparent width of the rasterscanned structure is d. **B** Sketch of an example of "tip broadening" of microtubules with a diameter of 30 nm, scanned by a tip with a radius 35 nm. At the bottom a resulting scan line is shown

The "tip broadening" can be calculated as follows:

$$d = 4 \times \sqrt{r \times R} \quad (1)$$

where d is the apparent width of a feature, which is approximated by a sphere of radius r and scanned by a tip with the radius R (Fig. 3).

From the measured widths of the microtubules (80–120 nm) we can calculate the effective radii of our AFM tips: 25–60 nm. However, lateral resolution depends on the overall height corrugation. On a flat periodic structure like a two-dimensional array of proteins, resolution can be better than 1 nm (Müller et al. 1995a). The same is true on top of a microtubule. Even when the tip broadening of the entire microtubule is severe, it is conceivable to resolve individual protofilaments on top of this broadened structure. On a flat surface, periodicities have to be reproduced exactly, no matter how large or small a tip is. However, on the curved surface of a microtubule the distance between adjacent protofilaments will also be distorted, as can be seen in Fig. 2.

The radius of AFM tips can be optimized by using electron beam deposited (ebd) tips (Keller et al. 1992). These tips are grown in the vacuum chamber of a scanning electron microscope by focusing the electron beam on top of a silicon nitride or silicon tip without scanning. Usually those tips, grown from residual pump oil in the chamber, are sharper than the silicon nitride or silicon tips. When imaging microtubules with ebd tips some longitudinal structures become visible (Fig. 2B–D). The number of these structures and their size indicate that they are the protofilaments (Fig. 2B, arrows). Some of the protofilaments stick up higher than the others. We think that the protofilaments became separated at the end of the microtubule. The protofilaments consisting of α- and β-tubulin subunits are about 4 nm in diameter. Our AFM images in buffer solution of the inner and outer part of the microtubules show that the inner surface is more corrugated than the outer one (Fig. 2C and D). The longitudinal rows can only be detected at the inner surface (Fig. 2D, arrows). As both surfaces have been raster scanned with the same tip, it can be discounted that the differences are due to different tip geometries. This has also been observed by high-resolution electron microscopy (Nogales et al. 1995). The profile of the α- and β-subunit of tubulin has been shown to be more rugged at the inside of the microtubule wall whereas at the outside the microtubules present a smoother surface (Nogales et al. 1997).

Another surface to adsorb microtubules onto can be created by the fusion of positively charged lipid vesicles (Zantl et al. 1999). After the fusion on the solid support a lipid bilayer is formed which in the case of DPDAP is in the crystalline phase, exposing a dense layer of positively charged headgroups. As the fusion takes place in deionized water and the imaging of microtubules has to be done in buffer solution, the characteristics of the surface change slightly. Small

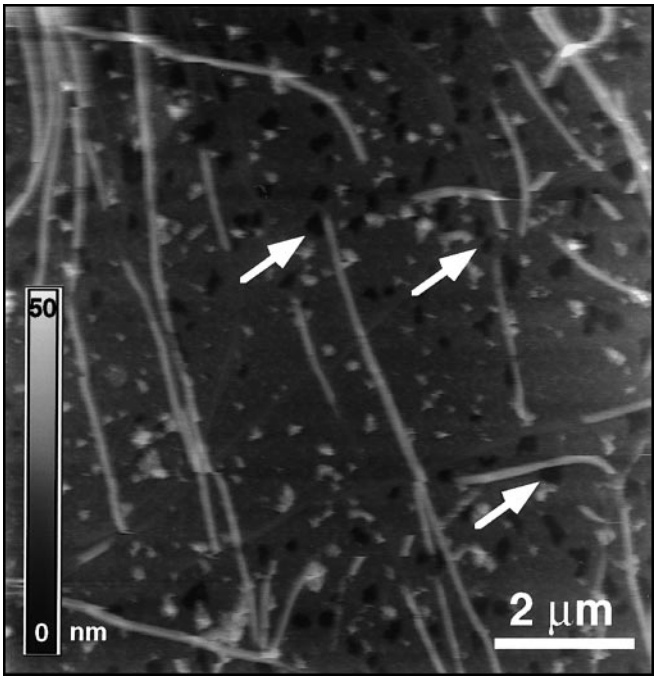

Fig. 4 Microtubules adsorbed onto DPDAP imaged in buffer solution by AFM. The imaging was done in tapping mode with a microlever. The height signal is shown. Note the holes in the DPDAP bilayer (*arrows*) where the microtubules do not adhere. The microtubules are not very strongly attached to the surface and only short parts can be imaged

defects appear in the lipid surface (Fig. 4, white arrows). The resulting lipid bilayer is a convenient surface to which the microtubules can adsorb, but it is much less stable than the silane surface. This is mainly due to the defects which grow over time.

The microtubules immobilized on the lipid surface exhibit the expected height of about 30 nm and are therefore presumably intact, but they are very short (Fig. 4). This might be due to defects where they fail to adsorb. Looping into the buffer volume might lead to their damage and/or braking during scanning. Further scanning leads to greater damage of the lipid layer and therefore also to damage of the microtubules.

When the support has a hydrophobic appearance like from outdated DETA surfaces, "sheets" appear (Fig. 5A). They are strongly attached to the support. These sheets are very flat (their height is about 4 nm) and have a width of about 100 nm, which can be seen clearly in the line plot where an intact microtubule is compared with a flat microtubule "sheet" (Fig. 5B). This appearance might be due to the splitting of the microtubule cylinder at a distinct seam, where the binding forces between the protofilaments are reduced (Mandelkow et al. 1986). The geometry of the imaged "sheets" in Fig. 5 fits very well the idea of the split microtubules lying flat on the support. As we have never seen any substructure on those "sheets" it might be possible that the adsorption on the hydrophobic surface leads to the denaturing of tubulin.

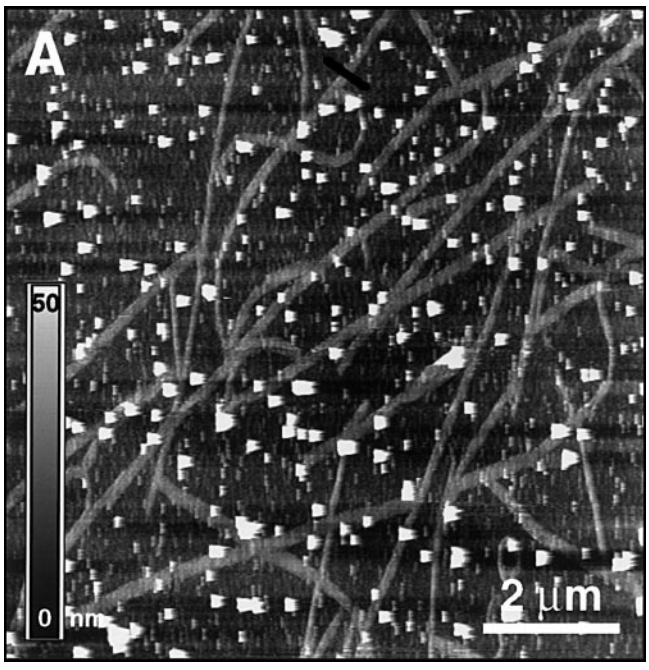

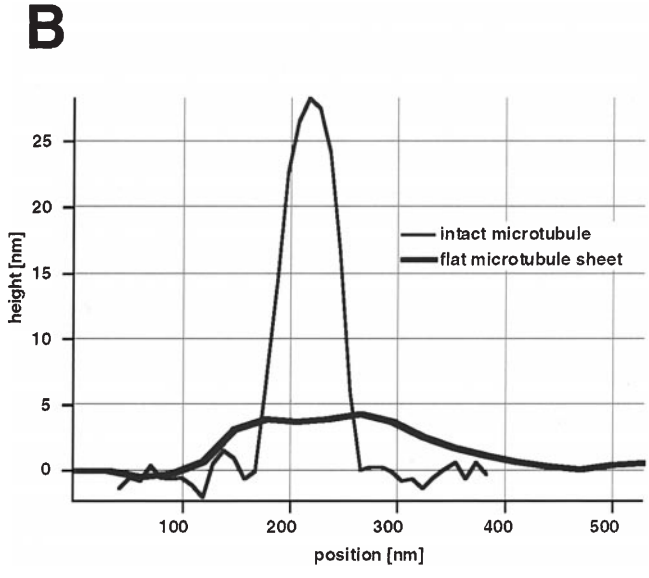

Fig. 5A, B Microtubules adsorbed onto outdated DETA imaged in buffer solution by AFM. The images show the error signal. The imaging was done in tapping mode with a microlever. **A** The elongated structures do have a flat appearance and the width is about 100 nm, corresponding to a cylinder opened at a seam and pressed down by interaction forces to a surface. The height of the flat "microtubules" is 4 nm, which is the diameter of a tubulin monomer. The *black bar* in the upper middle section shows the line for the line plot in **B**. **B** Line plot of an intact microtubule (*thin line*) and a flat microtubule "sheet" (*bold line*)

Microtubules can be decorated with kinesin and imaged by AFM in buffer solution

When kinesin molecules are incubated with microtubules in the presence of the non-hydrolyzable ATP analog AMP-PNP, it binds irreversibly to the microtu-

bules (Hirose et al. 1995). The kinesin-decorated microtubules adsorb very tightly to DETA-coated cover glasses (Fig. 6). As the ratio of kinesin to tubulin during incubation was 1:10, the microtubules are covered with kinesin molecules (Fig. 6, white arrows). The decoration of the microtubules with kinesin molecules makes visible the pitch of the tubulin monomers in the polymer. The elongated substructure of the protofilaments disappears and cross stripes appear with an angle of about 10–20° to the normal of the microtubule axis. Kinesin molecules bind to one tubulin dimer and seem to be concentrated over one monomer (Kikkawa et al. 1995), the β-subunit (Hoenger et al. 1998).

One prerequisite for imaging motor protein activity is the stability of the proteins adsorbed to the solid support (Radmacher et al. 1994; Fritz et al. 1995b). To test the stability, kinesin-decorated microtubules have been adsorbed on DETA-coated cover glasses (Fig. 7). In order to obtain to a reasonable scan speed the resolution of the image has to be reduced to 128 × 128 pixels. With a scan speed of 100 Hz this results in 1.3 s per image. As can be seen in Fig. 7, the kinesin appears as small "blobs" on the microtubules. These "blobs" and the microtubules can be imaged very stably even at this high scan speed (the usual scan speed for high resolution is on the order of a few hertz). There is no distortion detectable and each structure on an image appears also on the next one. Only a small drift can be observed (e.g. for comparison: Fig. 7A and L, arrows). This shows that it is possible to image kinesin-decorated microtubules for a long time without any damage. Our following experiments will be to directly observe the movement of kinesin along microtubules with the AFM in order to find out how kinesin molecules move over the microtubules and obtain some evidence about the chemomechanical coupling.

Fig. 7A–L Movie of kinesin-decorated microtubules over 30 s. The imaging was done in tapping mode with a silicon nitride cantilever with oriented twin tips. **A–L** Subsequent images of kinesin decorated microtubules in buffer solution. The kinesin was bound in the presence of AMP-PNP to the microtubules. Each image consists of 128 × 128 pixels. The imaging speed was 100 Hz, resulting in 1.3 s per image. Only those images were taken where the area was scanned from top to bottom, resulting in a gap between the images of 1.3 s. A small drift of the image can be seen (e.g. note the structure at the *arrow* in **A** and **L**)

Fig. 6A, B Microtubules decorated with kinesin adsorbed on a DETA-coated cover glass. The imaging was done in tapping mode with a silicon nitride cantilever with oriented twin tips. **A** Height image of kinesin-decorated microtubules in buffer solution. The kinesin attached to the microtubules appears as small globular "blobs". **B** Parallel error signal of **A**. The fine corrugations on that image show stripes running perpendicular to the microtubule polymer (*white arrows*). This indicates the lining-up of the tubulin subunits (in this case the angle is on the order of 10–20°) which are now more pronounced than the protofilaments (Fig. 2) owing to the decoration with kinesin

Conclusions

We used several different substrates and different buffer solutions to immobilize single protein molecules (Table 2). Microtubules especially do need a very defined substrate with a high density of positive charges. The buffer conditions for imaging turned out to be useful in the range of 50 mM PIPES but we did only vary the ionic strength between 50 and 80 mM PIPES. The ten-

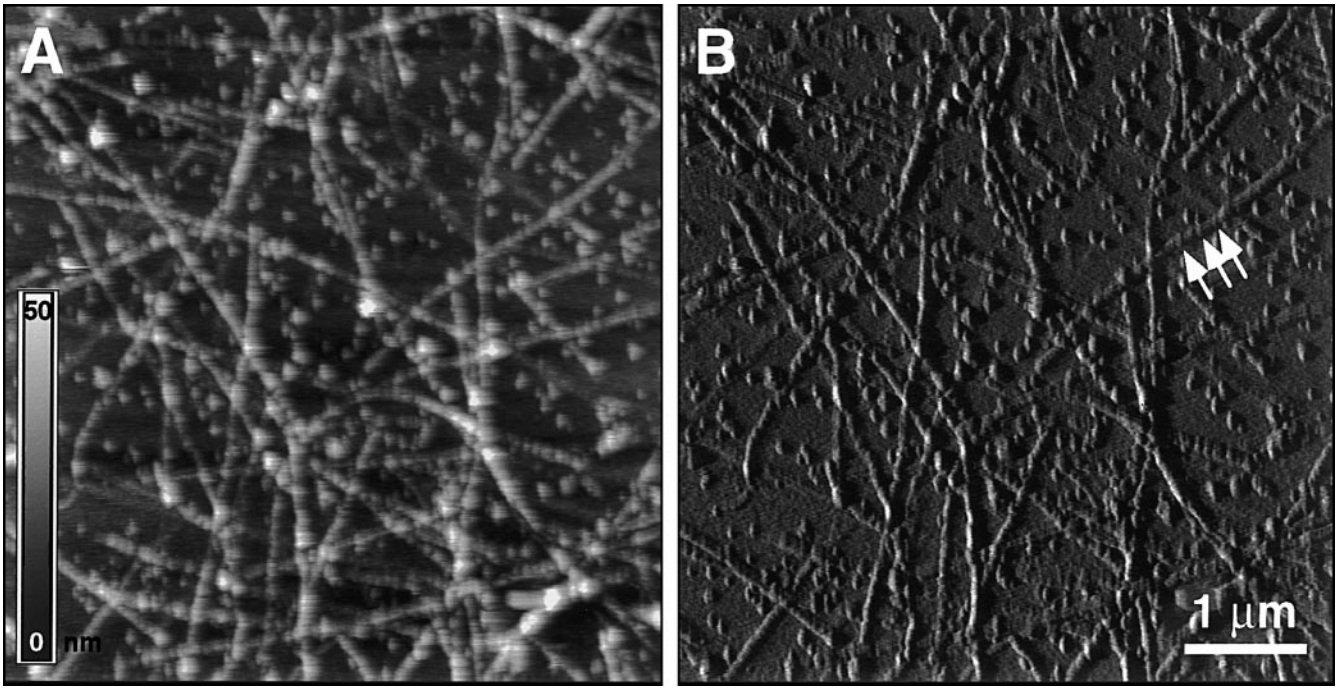

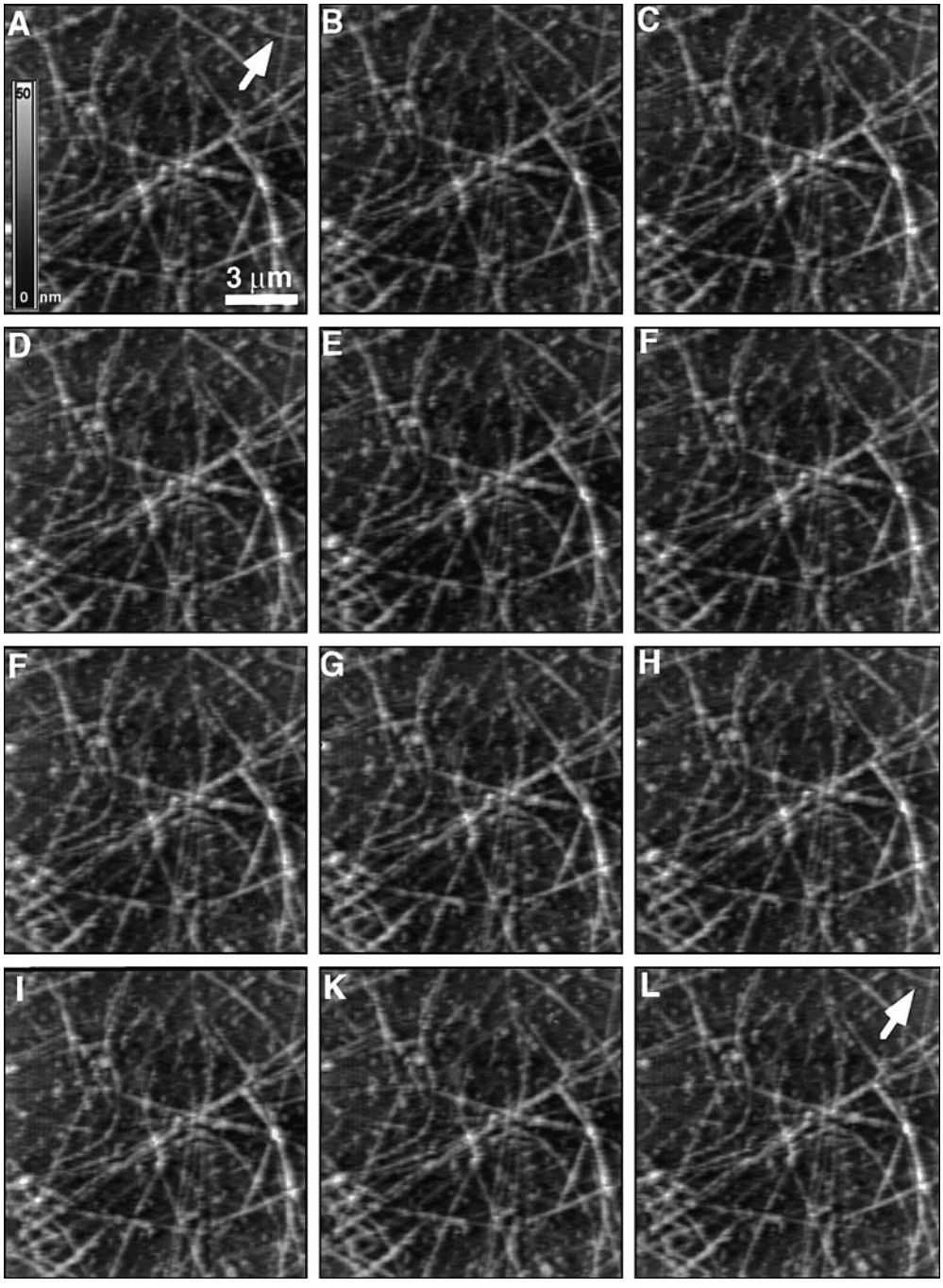

Table 2 Substrate and buffer conditions for the adsorption of microtubules

Protein	Substrate	Buffer conditions	Appearance
Microtubules	Mica	PEM 50	No adsorption
Microtubules	OTS	PEM 50	No adsorption
Microtubules	DMS	PEM 50	No adsorption
Microtubules	DETA	PEM 80	Weak adsorbed microtubules
Microtubules	DETA	PEM 50	Intact microtubules
Microtubules	DPDAP	PEM 50	Short microtubules
Microtubules	DETA outdated	PEM 50	Flat microtubule "sheets"

dency is very clear: the lower the ionic strength, the better is the immobilization of the microtubules and the better is the resolution. The same substrate and buffer conditions could be used for kinesin-decorated microtubules.

We have shown that native microtubules and native kinesin-decorated microtubules can be imaged stably in buffer solution with a lateral resolution up to about 5 nm. It is conceiveable that the lateral resolution can be further increased by using plasma etched ebd tips (Wendel et al. 1995). The vertical resolution is a few ångstrøm and therefore gives us the subject for our next experiments: imaging the movement of kinesin directly.

Acknowledgements We very much thank Prof. E. Sackmann for fruitful discussions and his kind support. We thank Roman Zantl for the preparation of the lipid bilayers. This work was supported by the Deutsche Forschungsgemeinschaft (I.W., C.M.K., M.R., M.F.) and the National Science Foundation grant NSF DMR 9622169 (P.K.H.).

References

Bezanilla M, Drake B, Nudler E, Kashlev M, Hansma PK, Hansma HG (1994) Motion and enzymatic degradation of DNA in the atomic force microscope. Biophys J 67: 1–6

Bezanilla M, Manne S, Laney DE, Lyubchenko YL, Hansma HG (1995) Adsorption of DNA to mica, silylated mica and minerals: characterization by atomic force microscopy. Langmuir 11: 655–659

Binnig G, Quate CF, Gerber C (1986) Atomic force microscope. Phys Rev Lett 56: 930

Block SM (1997) Real engines of creation. Nature 386: 217–219

Bloom GS, Endow SA (1994) Motor proteins 1: kinesins. Protein Profile 1: 1059–1106

Bloom GS, Wagner MC, Pfister KK, Brady ST (1988) Native structure and physical properties of bovine brain kinesin and identification of the ATP-binding subunit polypeptide. Biochemistry 27: 3409–3416

Brinkley WBR (1997) Microtubules: a brief historical perspective. J Struct Biol 118: 84–86

Fritz M, Radmacher M, Gaub HE (1994) Granula motion and membrane spreading during activation of human platelets imaged by atomic force microscopy. Biophys J 66: 1328–1334

Fritz M, Radmacher M, Allersma M, Cleveland J, Stewart R, Hansma P, Schmidt C (1995a) Imaging microtubules in buffer solution using tapping mode atomic force microscopy. Proc SPIE 2384: 150–157

Fritz M, Radmacher M, Cleveland JP, Gieselmann R, Allersma MW, Stewart RJ, Schmidt CF, Hansma PK (1995b) Imaging globular and filamentous proteins in physiological buffer solution in tapping mode atomic force microscopy. Langmuir 11: 3529–3535

Hansma PK, Cleveland JP, Radmacher M, Walters DA, Hillner PE, Bezanilla M, Fritz M, Vie D, Hansma HG, Prater CB, Massie J, Fukunaga L, Gurley J, Elings V (1994) Tapping mode atomic force microscopy in liquids. Appl Phys Lett 64: 1738–1740

Hirokawa N (1998) Kinesin and dynein superfamily proteins and the mechanism of organelle transport. Science 279: 519–5265

Hirose K, Lockhart A, Cross RA, Amos LA (1995) Nucleotide-dependent angular change in kinesin motor domain bound to tubulin. Nature 376: 277–279

Hoenger A, Sack S, Thormählen M, Marx A, Müller J, Gross H, Mandelkow E (1998) Image reconstructions of microtubules decorated with monomeric and dimeric kinesins: comparison with X-ray structure and implications for motility. J Cell Biol 141: 419–430

Hoh JH, Schoenenberger C-A (1994) Surface morphology and mechanical properties of MDCK monolayers by atomic force microscopy. Biophys J 107: 1105–1114

Hoh J, Sosinsky GE, Revel J-P, Hansma PK (1993) Structure of the extracellular surface of the gap junction by atomic force microscopy. Biophys J 65: 149–163

Hyams JS, Lloyd CW (1994) Microtubules. Wiley-Liss, New York

Karrasch S, Dolder M, Schabert F, Ramsden J, Engel A (1993) Covalent binding of biological samples to solid supports for scanning probe microscopy in buffer solution. Biophys J 65: 2437–2446

Karrasch S, Hegerl R, Hoh JH, Baumeister W, Engel A (1994) Atomic force microscopy produces faithful high-resolution images of protein surfaces in an aqueous environment. Proc Natl Acad Sci USA 91: 836–838

Keller D, Deputy D, Alduino A, Luo K (1992) Sharp, vertical-walled tips for SFM imaging of steep or soft samples. Ultramicroscopy 42–44: 1481–1489

Kikkawa M, Ishikawa T, Wakabayashi T, Hirokawa N (1995) Three-dimensional structure of the kinesin head-microtubule complex. Nature 376: 274–276

Mandelkow E-M, Schultheiss R, Rapp R, Müller M, Mandelkow E (1986) On the surface lattice of microtubules: helix starts, protofilament number, seam, and handedness. J Cell Biol 102: 1067–1073

Metoz F, Wade RH (1997) Diffraction by helical structures with seams: microtubules. J Struct Biol 118: 128–139

Müller DJ, Büldt G, Engel A (1995a) Force-induced conformational change of bacteriohodopsin. J Mol Biol 249: 239–243

Müller DJ, Schabert FA, Büldt G, Engel A (1995b) Imaging purple membranes in aqueous solutions at sub-nanometer resolution by atomic force microscopy. Biophys J 68: 1681–1686

Nogales E, Wolf SG, Khan I, Luduena RF, Downig KH (1995) Structure of tubulin at 6.5 Å and location of the taxol-binding site. Nature 375: 424–427

Nogales E, Wolf SG, Downing KH (1997) Visualizing the secondary structure of tubulin: three-dimensional map at 4 Å. J Struct Biol 118: 119–127

Radmacher M, Tillmann RW, Fritz M, Gaub HE (1992) From molecules to cells – imaging soft samples with the AFM. Science 257: 1900–1905

Radmacher M, Fritz M, Hansma HG, Hansma PK (1994) Direct observation of enzyme activity with the atomic force microscope. Science 265: 1577–1579

Radmacher M, Fritz M, Kacher CM, Cleveland JP, Hansma PK (1996) Measuring viscoelastic properties of human platelets with the atomic force microscope. Biophys J 70: 556–567

Schabert FA, Rabe JP (1996) Vertical dimension of hydrated biological samples in tapping mode scanning force microscopy. Biophys J 70: 1514–1520

Svoboda K, Schmidt CF, Schnapp BJ, Block SM (1993) Direct observation of kinesin stepping by optical trapping interferometry. Nature 365: 721–727

Thormählen M, Marx A, Müller SA, Song Y-H, Mandelkow E-M, Aebi U, Mandelkow E (1998) Interaction of monomeric and dimeric kinesin with microtubules. J Cell Biol 141: 419–430

Vale RD, Reese TS, Sheetz MP (1985) Identification of a novel force-generating protein, kinesin, involved in microtubule-based motility. Cell 42: 39–50

Vinckier A, Heyvaert I, D'Hoore A, McKittrick T, Van Haesendonck C, Engelborghs Y, Hellemans L (1995) Immobilizing and imaging microtubules by atomic force microscopy. Ultramicroscopy 57: 337–343

Wade RH, Hyman AA (1997) Microtubule structure and dynamics. Curr Opin Cell Biol 9: 12–17

Wendel M, Lorenz H, Kotthaus JP (1995) Sharpened electron beam deposited tips for high resolution atomic force microscope lithography and imaging. Appl Phys Lett 67: 3732–3734

Williams RCJ, Lee JC (1982) Preparation of tubulin from brain. Methods Enzymol 85: 376–385

Yang JT, Saxton WM, Stewart RJ, Raff E, Goldstein LSB (1990) Evidence that the head of kinesin is sufficient for force generation and motility in vitro. Science 249: 42–47

Yang J, Tamm LK, Tillack TW, Shao Z (1993) New approach for atomic force microscopy of membrane proteins – the imaging of cholera toxin. J Mol Biol 229: 286–290

Zantl R, Artzner F, Rapp G, Rädler JO (1999) Thermotropic structural changes of saturated-cationic-lipid-DNA complexes. Europhys Lett 45: 90–96